Structural Dependence of Protic Ionic Liquids on Surface, Optical, and Transport Properties

ARTICLE *in* JOURNAL OF CHEMICAL & ENGINEERING DATA · MAY 2015

Impact Factor: 2.04 · DOI: 10.1021/acs.jced.5b00077

2 AUTHORS:

Pratap Chhotaray

Indian Institute of Technology Madras

9 PUBLICATIONS **123** CITATIONS

SEE PROFILE

Ramesh L Gardas

Indian Institute of Technology Madras

109 PUBLICATIONS **2,771** CITATIONS

SEE PROFILE

Journal of chemical & engineering data

Article

pubs.acs.org/jced

Structural Dependence of Protic Ionic Liquids on Surface, Optical, and Transport Properties

Pratap K. Chhotaray and Ramesh L. Gardas*

Department of Chemistry, Indian Institute of Technology Madras, Chennai, 600 036, India

Supporting Information

ABSTRACT: We report a systematic study to understand the structural dependence of protic ionic liquids, having ammonium or hydroxylammonium as cation and carboxylate as anion, on surface, optical, and transport properties. Experimental measurements of surface tension, refractive index, and electrical conductivity were investigated in the temperature range from (293.15 to 333.15) K at atmospheric pressure to understand the effect of the hydroxyl group on the cationic part and alky chain length and inclusion of highly electronegative fluorine atoms on the anionic part of studied protic ionic liquids. Further, surface entropy, surface energy, critical temperature, parachor, molar refraction, electronic polarizability, thermo-optic coefficient, and free volume were estimated from experimental values. Experimental electrical conductivity data were correlated using the Vogel−Tammann−Fulcher equation. The ionicity was assessed on the basis of the fractional Walden rule, and it was found that the studied protic ionic liquids fall below the ideal line. Upon hydroxyl group functionalization on the cationic chain length, the surface tension and refractive index of ionic liquids increase significantly, whereas the electrical conductivity decreases over the nonfunctionalized ionic liquid counterpart. Moreover, experimental and calculated results were explained to understand the effect of temperature and moiety of ionic liquid on studied thermophysical properties.

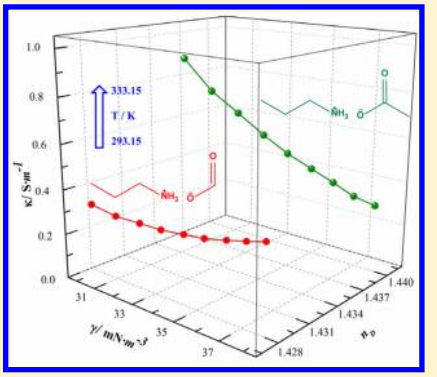

1. INTRODUCTION

It seems that the search for a new smart solvent has achieved a major breakthrough in the form of ionic liquid (IL). As the name suggests, generally ILs are composed of ions, which play an important role in their applicability and utility. The inherent potential of ILs lies in their ability to be tailored to accomplish a specific requirement of industry or academic research.[1] The ILs outstanding thermophysical properties make them promising in diverse applications such as reaction media as well as catalyst, heat and mass transfer media, electrochemical application, cellulose processing and so forth.[2−4] Although ILs are broadly classified as protic ionic liquid (PIL) and aprotic ionic liquid (AIL), as research progressed, several new names were proposed for ILs, depending upon the synthetic procedure, behavior, and applications, which may include switchable ionic liquid (SIL),[5] task specific ionic liquid (TSIL),[6] and brønsted acidic ionic liquid, etc.[7]

To date, AILs have received by far more attention than PILs. However, in recent years PILs have drawn the interest of the scientific community due to their easy method of preparation and presence of transferable proton along with several other properties. Potential applications of PILs because of their unique properties include media and/or catalyst in organic synthesis, chromatography, fuel cell, lignin dissolution, and self-assembly media.[8−12]

So far the adequate thermophysical characterization of PILs is limited possible because of their diversity or fast growth, therefore the study of thermophysical properties of PILs is of great importance mainly for two reasons. First, it will facilitate the production and process design for industrial applications of ionic liquids and second, the knowledge of the thermophysical properties is necessary to develop quantitative structure−property relationship (QSPR) models and empirical equations.[13−15] In fact, a QSPR model has the capability to predict the rational determination of various thermophysical properties without even synthesizing ILs. Moreover, as there is a growing demand for functionalized ILs for specific application, it is necessary to know the thermophysical properties of existing ILs.[16]

Temperature-dependent surface tension studies are a basic requirement for liquid state modeling and many practical applications such as distillation, extraction, absorption, and adsorption.[17,18] Also, surface tension data can be used to account for the solvation capacity of ILs, as solubility not only depends upon the energy of solvation but is also governed by the interfacial tension of the solute and solvent. Atkin et al. investigated the surface of PILs by the method of like X-ray reflectivity which reveals that hydrophobicity and hydrogen bonding in PILs determine the sharpness of segregation and extent of ordering at the interface, respectively.[19] The high refractive index of ILs makes them a good candidate to be used as new optical materials for many applications. For instance, to

Received: January 22, 2015
Accepted: May 5, 2015

DOI: 10.1021/acs.jced.5b00077
J. Chem. Eng. Data XXXX, XXX, XXX−XXX

locate inclusions nondestructively, in unpolished diamonds and other minerals by optical means, it is desirable to immerse these minerals in a fluid with the same refractive index.[20] Unfortunately, the available materials such as AsI_3 (n_D = 2.2) or SnI_4 (n_D = 2.1) are solid at room temperature, poisonous, unstable, and extremely unpleasant. Because the ILs are green solvents, by tuning the cations/anions they can be used as a potential immersion fluid in mineralogical studies. Temperature-dependent electrical conductivity is considered by far the most important transport property in the context of ILs as it is essential for any electrochemical process. The extreme interest of application includes ILs as an electrolyte in electrochemistry and in electrochemical devices such as lithium ion batteries, double layer capacitors, fuel cells, and photoelectrochemical cells.[21−24]

At this juncture, as a follow-up study of our previous work,[25] we studied the surface tension, refractive index, and electrical conductivity of five protic ionic liquids with an amino functional group, namely, propylammonium formate (PAF), propylammonium acetate (PAAc), 3-hydroxypropylammonium formate (3HPAF), 3-hydroxypropylammonium acetate (3HPAAc), and 3-hydroxypropylammonium trifluoroacetate (3HPATFAc). These ILs were selected because recently ammonium and hydroxylammonium ILs have drawn considerable attention for CO_2 absorption from both natural and flue gas.[26−28] The presence of polar −OH groups in hydroxylammonium ILs makes them suitable for solvation of polar solvents, and they can also solubilize many polymers such as polyaniline, polypyrrole, and zein (an industrially important natural polymer).[29,30] Moreover, it is evident that carboxylate-based ILs are suitable for cellulose and lignocellulose dissolution.[31,32] The high hydrogen-bond basicity (Kamlet−Taft parameter, β) of the carboxylate ion, which can strongly coordinate with the hydroxyl group of carbohydrates is the guiding factor for cellulose dissolution.[33]

To the best of our knowledge no systematic study over the range of temperature for the above-mentioned PILs has been reported in the literature except by Hou et al.[34] and Pinkert et al.[35] While Hou et al.[34] studied the refractive index and electrical conductivity of PAAc at 298.15 K, Pinkert et al.[35] studied only the electrical conductivity of 3HPAF and 3HPAAc at (298.15, 308.15, 318.15, and 328.15 K) at 10 K interval. As temperature-dependent thermophysical property studies are important for both practical application and modeling of the liquid state, we have measured the properties at different temperatures ranging from (293.15 to 333.15) K with an interval of 5 K, at atmospheric pressure. The experimental surface tension values were used to calculate the surface thermodynamic functions (surface entropy, surface energy) and parachor. The critical and boiling temperatures were also estimated by using the Guggenheim and Eötvos formula. Furthermore, free volume, molar refraction, and molar conductivity values were estimated from refractive index and electrical conductivity data points, respectively. Electrical conductivity results permit us to evaluate the ionicity of studied PILs based on a Walden plot. Moreover, these temperature and structural dependence studies enabled us to have an insight on the overall behavior of PILs.

2. EXPERIMENTAL SECTION

2.1. Materials Used for the Synthesis of PILs. The details of source and purity of chemicals used for the synthesis of the PILs have been presented in Table 1 and were used without further purification. The typical synthetic procedure adopted for the synthesis of the PILs has been described in detail in our previous work.[25] Generally equimolar acids were added dropwise to the double-necked round-bottom flask containing base, equipped with a reflux condenser. The flask was kept under ice bath with vigorous stirring. After the addition was completed, the stirring was continued for another 24 h under nitrogen atmosphere. Further, the viscous sample was kept under high vacuum to remove the excess starting materials if any and then subjected to NMR analysis. The proton NMR data of all the studied PILs were given in the Supporting Information.

Table 1. Specifications of the Chemicals Used

name	purity[a]	source
formic acid	≥ 95 %	Sigma-Aldrich
acetic acid	99 %	Sigma-Aldrich
trifluoroacetic acid	99 %	Sigma-Aldrich
propyl amine	≥ 99 %	Sigma-Aldrich
3-amino-1-propanol	99 %	Sigma-Aldrich

[a]All chemicals were used as received from the source, without further purification.

2.2. Methods and Measurements. Surface tensions of the pure PILs were measured by using a Dataphysics tensiometer (DCAT 11 EC) using the du Noüy ring (made up of platinum) as the probe. Measurement, analysis, and control were carried out by SCAT 31 software. It can measure surface tension from 1 to 1000 mN·m^{-1} with a resolution of ± 0.001 mN·m^{-1}. The external temperature was controlled by a Julabo water bath (ΔT = ± 0.1 K), and the sample holder temperature was maintained by a Pt 100 sensor with an accuracy of ± 0.01 K. The method involves the maximum force necessary to detach the platinum ring from the surface of the liquid. The maximum force on the ring due to the resistance of the fluid is proportional to the surface tension as given by

$$\gamma = \frac{F_{max}B}{4\pi R} \quad (1)$$

where γ is the surface tension, F_{max} is the maximum force exerted on the ring, B is the instrument correction factor that accounts for the geometry at the interface about the ring, and R is the diameter of the ring. The instrument was calibrated daily by measuring the surface tension of Millipore water. Measurements were carried out under nitrogen atmosphere to avoid contamination with atmospheric moisture. An electrical conductivity measurement was performed by a Eutech (PC 700) instrument that includes an electrode with a cell constant of k = 1 and built in temperature sensor. The conductance cell was calibrated with the aqueous solution of 0.01 N KCl, and the cell can measure conductivity from 0.0 μS to 200 mS. A nitrogen atmosphere was maintained throughout the measurement by using an in-house fabricated double layered glass jacket setup. The inlet and outlet of the setup were connected to the water bath for temperature maintenance. Refractive indices were measured using an Abbemat 300 refractometer from Anton Paar. It can measure a refractive index from 1.3 n_D to 1.72 n_D using the yellow line of sodium (λ = 589.3 nm) with an accuracy of ± 0.0001 n_D. The measuring prism used is made of YAG (Tttrium−Aluminum−Garnet), and the measuring area is made of stainless steel. The instrument has a built-in dual Peltier controller which allows measurement from 10 °C to 85 °C with a maximum deviation of 0.005 °C. The apparatus was

DOI: 10.1021/acs.jced.5b00077
J. Chem. Eng. Data XXXX, XXX, XXX−XXX

calibrated by Millipore water every day prior to the experiment, and the accuracy was checked with the refractive index of known solvents. A Karl Fischer Titrator from Analab (Micro Aqua Cal 100) was used to measure the water content of the ILs. It operates on the conductometric titration principle using a dual platinum electrode, which can enable the detection of water content from less than 10 ppm to 100 %. The instrument was calibrated with Millipore quality water. Before each measurement the samples were kept under high vacuum to remove the moisture, and the water content was found to be less than 3395 ppm for PAF, 3732 ppm for PAAc, 3859 ppm for 3HPAF, 4158 ppm for 3HPAAc, and 3684 ppm for 3HPATFAc. Further vacuum drying was avoided as it may lead to the proton back transfer as well as decomposition. Each measurement was carried out in triplicate, and the average values are reported here. The standard uncertainties associated with the measurements were estimated to be less than 0.11 $mN{\cdot}m^{-1}$, 0.5 %, and 0.0003 for surface tension, electrical conductivity, and refractive index, respectively.

3. RESULTS AND DISCUSSION

For studied five PILs, the measured experimental values of surface tension, refractive index, and electrical conductivity from (293.15 to 333.15) K and at atmospheric pressure are illustrated in Table 2. The density and viscosity values used for the calculation of derived thermodynamic properties were taken from our previous work.[25]

3.1. Surface Tension. Different from molecular liquids, for the the ILs in which the nanoscale segregation predominates and is nonisotropic from a structural point of view, surface tension is a complex combination of several interactions involving long-range coulomb forces, short-range van der Waals, and hydrogen-bonding forces.[17,36] According to Langmuir's principle of independent surface action, it is the part of the interacting molecules which are present at the interface that are responsible for surface tension.[37] The measured values shown in Table 2, indicate that both cation and anion have influence on the surface tension, these results are in good agreement with observations made by Santos et al.[36] which states that both cations and anions occupy the same plane at the gas−liquid interface. As can be seen from Table 2, the surface tension values are well above those of molecular solvents, for instance methanol (22.07 $mN{\cdot}m^{-1}$), acetone (23.5 $mN{\cdot}m^{-1}$) and those of *n*-alkanes but still lower than that of water (71.98 $mN{\cdot}m^{-1}$).[38] In most of the organic compounds, the surface tension increases with an increase in the size of the molecule. On the contrary, the experimental result shows that the surface tension decreases from formate (PAF, 3HPAF) to acetate (PAAc, 3HPAAc) ILs with an increase in the alkyl chain length on the anion. The observed trends are in agreement with the results found by Watson and Law[39] using the direct recoil spectrometry (DRS) technique and molecular dynamics simulation by Jiang et al.[40] A molecule at the surface orients itself in such a way to keep the surface energy at a minimum, therefore energetically the most favorable orientation is that in which the charged groups are always located toward the bulk liquid and the alkyl group is always exposed to the gas phase.[41] ILs structures are broadly classified, as if the IL consists of a negatively/positively charged headgroup and uncharged alkyl chain tail group. As the chain length increases, the polar group of ILs shifts away from the surface, which causes the polarity of the surface to become weaker, which results in a decrease in surface tension. Upon the substitution of the hydroxyl group at the terminal carbon chain of the cation, the surface tension at 298.15 K increases from PAF (37.4 $mN{\cdot}m^{-1}$) to 3HPAF (56.4 $mN{\cdot}m^{-1}$) and for PAAc (33.1 $mN{\cdot}m^{-1}$) to 3HPAAc (47.5 $mN{\cdot}m^{-1}$). This substantial increase in the surface tension due to the functionalization of the terminal position of an alkyl chain can be interpreted by taking into account that the hydroxyl group decreases the ability of the alkyl chains to be segregated toward the surface and will interact more effectively via their exposed polar network.[42] These findings are also observed by Ghatee et al. In the functionalization from ethylammonium formate (EAF) to 2-hydroxyethylammonium formate (2HEAF), the surface tension at 303.15 K shot up from (38.5 to 70.1) $mN{\cdot}m^{-1}$.[43] Among the functionalized ILs, 3HPATFAc shows the least value of surface tension. This might be due to the presence of three electronegative fluorine atoms on the anion that reduces the hydrogen bonding tendency, which by far is considered as the most important interaction in ILs.[44]

Table 2. Surface Tension (γ), Refractive Index (n_D), Molar Refraction (R_m), Polarizability (α_e), and Electrical Conductivity (κ) of PAF, PAAc, 3HPAF, 3HPAAc, and 3HPATFAc from (293.15 to 333.15) K at Pressure p = 0.1 MPa

T/K	PAF	PAAc	3HPAF	3HPAAc	3HPATFAc
			$\gamma/mN{\cdot}m^{-1}$		
293.15	37.8	33.5	56.9	48.0	38.2
298.15	37.4	33.1	56.4	47.5	37.8
303.15	37.0	32.7	55.9	47.0	37.4
308.15	36.6	32.2	55.4	46.5	37.0
313.15	36.2	31.8	54.9	46.0	36.5
318.15	35.8	31.4	54.4	45.5	36.1
323.15	35.4	31.0	54.0	45.0	35.7
328.15	35.0	30.6	53.5	44.5	35.3
333.15	34.6	30.2	53.0	44.0	34.9
			n_D		
293.15	1.4400	1.4383	1.4678	1.4663	1.4113
298.15	1.4386	1.4369	1.4667	1.4652	1.4101
		1.4405[a]			
303.15	1.4372	1.4356	1.4655	1.4640	1.4090
308.15	1.4356	1.4341	1.4644	1.4628	1.4078
313.15	1.4341	1.4328	1.4632	1.4616	1.4067
318.15	1.4326	1.4313	1.4621	1.4605	1.4055
323.15	1.4310	1.4301	1.4610	1.4593	1.4044
328.15	1.4295	1.4287	1.4598	1.4581	1.4032
333.15	1.4280	1.4273	1.4586	1.4570	1.4020
			$\kappa/S{\cdot}m^{-1}$		
293.15	0.31	0.04	0.11	0.01	0.03
298.15	0.36	0.06	0.14	0.01	0.04
		0.04[a]	0.16[b]	0.01[b]	
303.15	0.44	0.08	0.17	0.01	0.06
308.15	0.51	0.10	0.21	0.02	0.09
			0.26[b]	0.03[b]	
313.15	0.59	0.14	0.26	0.02	0.12
318.15	0.68	0.17	0.30	0.03	0.16
			0.40[b]	0.05[b]	
323.15	0.78	0.22	0.36	0.04	0.20
328.15	0.87	0.27	0.42	0.05	0.25
			0.59[b]	0.09[b]	
333.15	1.00	0.33	0.49	0.06	0.31

[a]Reference 34. [b]Reference 35. Standard uncertainties u are $u(T)$ = 0.002 K, $u(\gamma)$ = 0.11 $mN{\cdot}m^{-1}$, $u(n_D)$ = 0.0003, $u(\kappa)$ = 0.5 %.

DOI: 10.1021/acs.jced.5b00077
J. Chem. Eng. Data XXXX, XXX, XXX−XXX

As an obvious behavior, Figure 1 depicts the linear decrease in surface tension for all PILs with increasing temperature.

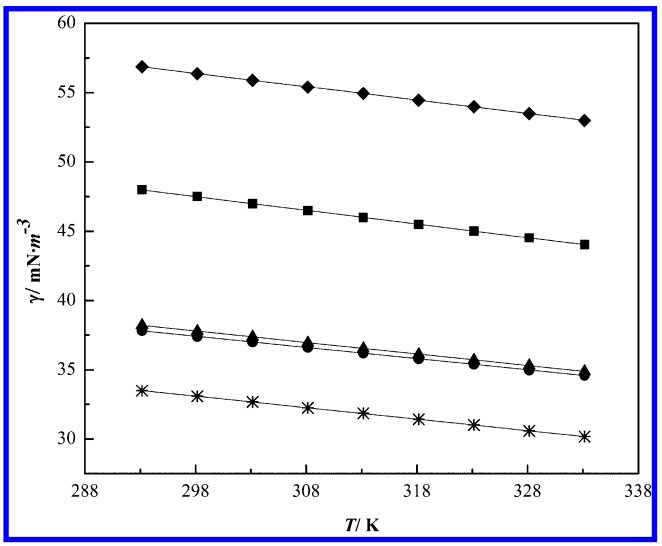

Figure 1. Experimental surface tension values of ionic liquids as a function of temperature from (293.15 to 333.15) K. ●, PAF; ∗, PAAc; ◆, 3HPAF; ■, 3HPAAc; ▲, 3HPATFAc. The symbols represent experimental values and the solid lines represent the values calculated from eq 2.

According to the thermodynamics of interface, the temperature dependence of surface tension values can be fitted to the following equation.[41]

$$\gamma = E^{S} + S^{S}T \tag{2}$$

where γ is the surface tension, E^{S} and S^{S} are fitting parameters and represent the surface energy and surface entropy, respectively. They can be represented as

$$E^{S} = \gamma - \left(\frac{d\gamma}{dT}\right)T \tag{3}$$

$$S^{S} = -\left(\frac{d\gamma}{dT}\right) \tag{4}$$

The values of surface thermodynamic properties along with average relative deviation (ARD) as given by eq 5 are illustrated in Table 3.

$$\mathrm{ARD} = \left(\frac{1}{n}\sum\frac{|\gamma_{exp} - \gamma_{cal}|}{\gamma_{exp}}\right)100 \tag{5}$$

Table 3. Surface Entropy (S^{S}) [eq 3], Surface Energy (E^{S}) [eq 4], Average Relative Deviation (ARD), Estimated Critical Temperatures (T_c) Using Both Eötvos (Eot) [eq 6] and Guggenheim (Gug) [eq 7] of Studied PILs

PILs	$S^{S}\cdot10^{3}$	E^{S}	ARD	T_c (Eot)	T_c (Gug)
	$mJ\cdot m^{-2}\cdot K^{-1}$	$mJ\cdot m^{-1}$		K	K
PAF	80.3	61.4	0.018	851	864
PAAc	82.6	57.7	0.015	773	784
3HPAF	96.7	85.2	0.014	990	1007
3HPAAc	99.3	77.1	0.021	854	880
3HPATFAc	82.8	62.5	0.021	841	853

where n is number of data points. It is noteworthy to mention here that compared to the organic compounds the surface entropies for the studied ILs are relatively low. This signifies a high surface organization even far better than the *n*-alkanes, which is considered as an example for surface organization.[45] These observations are also in good agreement with the results obtained for imidazolium ILs, by Lynden-Bell[46] through simulations and by Slouskin et al.[47] using X-ray reflectometry measurements. The observations indicate that a significant surface ordering exists in ILs, which causes the reduced surface entropy. Thus, it is not surprising that surface entropy increases with an increase in the size of the anion as shown in Table 3. On the other hand, the surface energy, seems to decrease with increasing alkyl chain length of anion in both the functionalized and nonfunctionalized PILs, probably due to the decrease in hydrogen-bond strength. An analogous behavior was also found by Freire et al. in which the surface energy values and trend of increasing alkyl chain length of cations of imidazoilum-based ILs match with that of ours.[48]

Critical and boiling temperatures are important relevant thermodynamic properties since they are used in corresponding states correlations describing equilibrium and transport properties.[49] Nevertheless, the experimental determination of these temperatures for ILs is a challenging task, as the ILs start to decompose while approaching the boiling point; therefore these temperatures can be only determined through empirical correlations. Rebelo et al.[50] proposed the use of the Eötvos[51] and Guggenheim[52] equations, respectively, to estimate the critical temperature of ILs by using the surface tension values as follows:

$$\gamma\left(\frac{M}{\rho}\right)^{2/3} = K(T_c - T) \tag{6}$$

$$\gamma = K\left(1 - \frac{T}{T_c}\right)^{11/9} \tag{7}$$

where M is molar mass, ρ is the density, T_c is the critical temperature, and K is the fitting parameter, also known as surface excess energy. As shown in Table 3, the critical temperatures obtained by both the empirical methods are not far from each other and follow the same trend as that of surface tension for PILs. The boiling point temperatures for PILs are also calculated from the equation developed by Rebelo et al.[50] as $T_b \approx 0.6T_c$ and reported in Table 4.

Recently, there has been considerable interest in the ionic liquid communities to estimate physicochemical properties by the semiempirical methods.[53,54] Even if the estimated results are quite far from the accurate physicochemical data, its significance is still very crucial. Among all the semiempirical

Table 4. Estimated Boiling Point from the Eötvos (Eot) [eq 6], Guggenheim (Gug) [eq 7], Difference in pK_a (ΔpK_a) and Slope of [eq 14] Representing Iconicity of Studied PILs

PILs	T_b (Eot) K	T_b (Gug) K	α	ΔpK_a
PAF	511	518	0.843	6.85
PAAc	464	471	0.838	5.84
3HPAF	594	604	0.826	6.21
3HPAAc	512	528	0.799	5.20
3HPATFAAc	505	512	0.950	9.73

DOI: 10.1021/acs.jced.5b00077
J. Chem. Eng. Data XXXX, XXX, XXX−XXX

Table 5. Parachor (P), Molar Volume (V_m), Molar Refraction (R_m), Electronic Polarizability (α_e), Free Volume (V_f), and Molar Conductivity (Λ) of Pure PAF, PAAc, 3-HPAF, 3-HPAAc, and 3-HPATFAc from (293.15 to 333.15) K

T		$V_m \cdot 10^6$	$R_m \cdot 10^6$	$\alpha_e \cdot 10^{-18}$	$V_f \cdot 10^6$	$\Lambda \cdot 10^5$
K	P	$m^3 \cdot mol^{-1}$	$m^3 \cdot mol^{-1}$	cm^3	$m^3 \cdot mol^{-1}$	$S \cdot m^2 \cdot mol^{-1}$
			PAF			
293.15	261.7	105.54	27.82	39.47	77.73	3.23
298.15	261.7	105.83	27.81	39.46	78.02	3.83
303.15	261.7	106.12	27.81	39.46	78.31	4.64
308.15	261.7	106.41	27.80	39.45	78.61	5.44
313.15	261.7	106.70	27.79	39.43	78.91	6.29
318.15	261.7	106.99	27.78	39.42	79.20	7.26
323.15	261.7	107.27	27.77	39.40	79.50	8.35
328.15	261.6	107.57	27.76	39.39	79.81	9.39
333.15	261.6	107.86	27.75	39.37	80.11	10.83
			PAAc			
293.15	289.5	120.37	31.62	44.86	88.75	0.51
298.15	289.5	120.74	31.63	44.87	89.11	0.70
303.15	289.6	121.12	31.64	44.89	89.48	0.95
308.15	289.5	121.50	31.65	44.90	89.85	1.26
313.15	289.5	121.88	31.66	44.92	90.22	1.67
318.15	289.5	122.27	31.67	44.94	90.60	2.13
323.15	289.5	122.66	31.69	44.96	90.97	2.66
328.15	289.4	123.05	31.70	44.98	91.35	3.26
333.15	289.3	123.44	31.71	45.00	91.73	4.09
			3HPAF			
293.15	289.7	105.50	29.31	41.59	76.18	1.15
298.15	289.7	105.72	29.32	41.60	76.41	1.46
303.15	289.7	105.95	29.32	41.60	76.63	1.84
308.15	289.7	106.17	29.32	41.60	76.86	2.26
313.15	289.7	106.40	29.32	41.60	77.08	2.74
318.15	289.6	106.63	29.32	41.60	77.31	3.24
323.15	289.6	106.85	29.32	41.60	77.53	3.84
328.15	289.6	107.08	29.31	41.59	77.76	4.54
333.15	289.5	107.30	29.31	41.59	77.99	5.28
			3HPAAc			
293.15	319.2	121.27	33.61	47.68	87.66	0.09
298.15	319.1	121.55	33.61	47.69	87.93	0.13
303.15	318.9	121.83	33.61	47.69	88.21	0.17
308.15	318.8	122.11	33.62	47.70	88.49	0.23
313.15	318.7	122.39	33.62	47.71	88.76	0.30
318.15	318.6	122.67	33.63	47.71	89.04	0.38
323.15	318.5	122.96	33.64	47.72	89.32	0.49
328.15	318.4	123.24	33.64	47.73	89.61	0.62
333.15	318.2	123.53	33.64	47.74	89.89	0.76
			3HPATFAc			
293.15	358.6	144.22	35.83	50.84	108.38	0.44
298.15	358.5	144.62	35.84	50.85	108.78	0.65
303.15	358.6	145.02	35.85	50.87	109.17	0.91
308.15	358.5	145.42	35.86	50.88	109.56	1.26
313.15	358.5	145.83	35.88	50.90	109.95	1.71
318.15	358.5	146.23	35.88	50.91	110.35	2.28
323.15	358.5	146.64	35.89	50.93	110.75	2.90
328.15	358.5	147.06	35.90	50.94	111.15	3.71
333.15	358.4	147.47	35.91	50.95	111.56	4.63

methods, the parachor (P) is the simplest and relatively oldest concept that is available as a link between the structure, density, and surface tensions of liquids.[55] The parachor was developed in 1924 by Sugden to predict physical properties of substances and can be defined using[56]

$$P = (M\gamma^{1/4})/\rho \quad (8)$$

where M is the molar mass, γ is the surface tension, and ρ is the density. Although, most of the studies on parachor have focused on the uncharged compound that does not include columbic interactions, there are many literature calculations of parachor for ILs. The values of parachor calculated using eq 8 are presented in Table 5. A plot of parachor versus temperature depicts a straight line parallel to the abscissa as shown in Figure

DOI: 10.1021/acs.jced.5b00077
J. Chem. Eng. Data XXXX, XXX, XXX−XXX

2, which validates the temperature independency of parachor (at least to first approximation) as observed in the literature.[57]

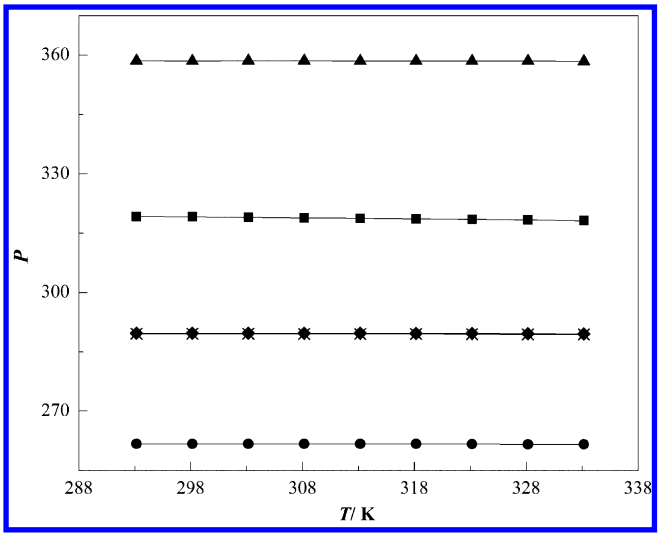

Figure 2. Plot of parachor (P) vs temperature for the studied PILs in the temperature range of (293.15 to 333.15) K. ●, PAF; ∗, PAAc; ◆, 3HPAF; ■, 3HPAAc; ▲, 3HPATFAc.

3.2. Refractive Index. As we can see from Figure 3, the refractive index covers a very narrow window (1.40 to 1.47)

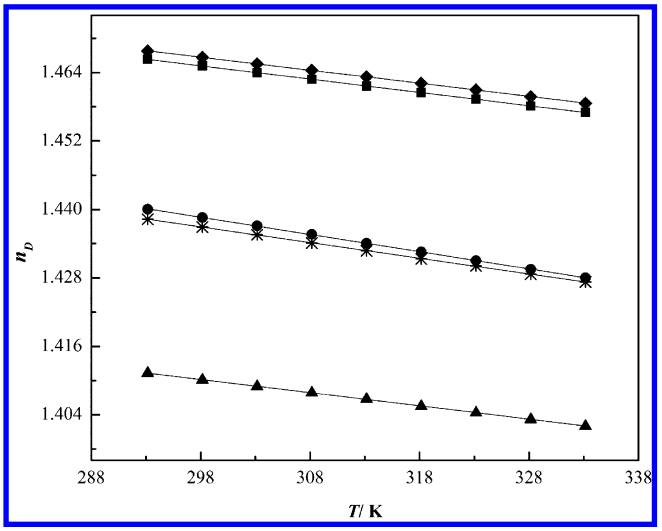

Figure 3. Experimental refractive index values of ionic liquids as a function of temperature from (293.15 to 333.15) K: ●, PAF; ∗, PAAc; ◆, 3HPAF; ■, 3HPAAc; ▲, 3HPATFAc. The symbols represent experimental values and the solid lines represent the values calculated from eq 9.

and decreases linearly over the studied temperature range and can be correlated to the following empirical equation as follows:

$$n_D = A_0 + A_1 T \quad (9)$$

where T is absolute temperature and A_0, A_1 are fitting parameters, reported in Table 6 along with ARD and are found to fit well within the experimental error. The fitting parameter A_1 is also known as the thermo-optic coefficient and it depends to some extent on the wavelength of incident light.[58] Generally for transparent materials, the thermo-optic coefficient value lies between (10^{-3} to 10^{-6}) K^{-1}, and the magnitude is an interplay between the thermal expansion coefficient and electronic polarizability in conjunction with other temperature-dependent changes in the refractive index that are less important in liquids.[59] Generally, thermo-optic coefficients are negative for materials possessing high thermal expansion because the thermal expansion is dominant nature over other factors, and our studied PILs also show negative values in the scale of 10^{-4}.

The measured refractive index values at 293.15 K are a little higher than some of those for common solvents like water (1.33), acetone (1.36), hexadecane (1.43), and ethanol (1.36). The refractive index decreases with increasing alkyl chain length of anion from PAF (1.4386) to PAAc (1.4369) and from 3HPAF (1.4667) to 3HPAAc (1.4652) at 298.15 K. Similar results were also found by Hong et al.[60] in which the refractive index decreases with an increase in the alkyl chain length of imidazolium cations. Functionalized ILs (3HPAF and 3HPAAc) show a higher index of refraction as compared to that of nonfunctionalized ILs (PAF and PAAc) as illustrated in Table 2. This could be attributed to the extra electron mobility around the additional −OH group of functionalized ILs, which is in good agreement with the results obtained by Muhammad et al.[61] and Tao et al.[62] for imidazolium- and cholinium-based ILs, respectively. The refractive index of PAAc at 298.15 K, which shows a relative deviation of 0.25 % with that reported by Hou et al.[34] (see Supporting Information, Figure S6) can be attributed to different water content and measurement technique involved.

The relationship between refractive index and several other physicochemical properties such as density and surface tension are of enormous importance and have been reported by several researchers.[60,63] The refractive index is an indication of the dielectric response to an external electric field induced by electromagnetic waves (light) and can be considered as the first order approximation response to electronic polarization within an instantaneous time scale. The Lorenz−Lorentz equation provides the relation between these two quantities given as follows:

Table 6. Fitting Parameters of Refractive Index [eq 9] and Electrical Conductivity [eq 12] along with Their Respective ARD

PILs	A_0	$A_1 \cdot 10^4$ / K^{-1}	ARD[a]·10^1	κ_0 / $S \cdot m^{-1}$	B / K	T_0 / K	ARD[b]
PAF	1.53	−3.02	0.020	132	1005	128	0.578
PAAc	1.52	−2.75	0.022	183	1030	170	0.582
3HPAF	1.54	−2.29	0.012	115	1016	147	0.587
3HPAAc	1.53	−2.33	0.013	148	1481	143	0.560
3HPATFAc	1.48	−2.30	0.018	168	929	185	0.447

[a]From eq 9. [b]From eq 12.

DOI: 10.1021/acs.jced.5b00077
J. Chem. Eng. Data XXXX, XXX, XXX−XXX

$$R_m = \frac{N_A \alpha_e}{3\varepsilon_0} = \frac{M}{\rho}\left(\frac{n_D^2 - 1}{n_D^2 + 2}\right) \quad (10)$$

where R_m is the molar refraction, N_A is the Avogadro's number, α_e is the molecular polarizability (electronic polarizability), ε_0 is the permittivity of free space, M is the molar masss, ρ is the density, and n_D is the refractive index. The molar refractions, generally considered for hard core molecular volumes are summarized in Table 5 along with molecular polarizability, for all studied ILs. The molar refraction values increase slightly with increasing temperature which indicates that the static polarizability is caused by the dispersion force of the ILs.[60]

Free volume (V_f) believed to be a key parameter determining the transport phenomena in ILs can be calculated as given by eq 11.[64,65]

$$V_f = V_m - R_m \quad (11)$$

where R_m is the molar refraction and V_m is the molar volume. Both are illustrated in Table 5 along with free volume. The free volume calculated by the above formula is generally applicable in the case of spherical molecules, yet this can be applicable to ILs which are made up of nonspherical ions, at least to draw a qualitative conclusion. It is observed that the free volumes increase with the addition of alkyl chain length to the anions. The refractive indices of the studied PILs decrease as the molar free volume increases, this observation is in good agreement with the literature values reported for the imidazolium type of ILs.[66] It is worth mentioning in the context of ILs that the so-called free volume can be related to the solubility of several gases and in particular to the low molecular weight CO_2, CH_4, and C_2H_6 gases.[67] An abundance of literature implies that the solubility of these gases increases if the free volumes in ILs are greater.[68,69] However, it should be noted that the mechanism of solvation of these nonpolar gases is more controlled by electrostatic specific interactions and only to some extent by free volume effects.[70]

The refractive index decreases significantly with increasing molecular weight from 3HPAAc (n_D = 1.4652 at 298.15 K, M = 135.16 g·mol^{-1}) to 3HPATFAc (n_D = 1.4101 at 298.15 K, M = 189.13 g·mol^{-1}). This is in agreement with Tariq et al.[71] and Fröba et al.[72] who found a strong dependence of anion molecular weight, which includes $[TFO]^-$, $[MeSO_4]^-$, $[EtSO_4]^-$, $[OAc]^-$, $[NTf_2]^-$, and $[N(CN)_2]^-$, on the refractive index of imidazolium- and phosphonium-based ILs. Refractive index is a measure of polarizability per unit volume; the higher molar volume in the case of 3HPATFAc ILs can also be attributed to its lower index of refraction. Moreover, the higher free volume of 3HPATFAc facilitates easy passage of the sodium D-line, which in turn has the lower refractive index as observed in the case of [EMIM]-based ILs reported by Hasse et al.[66]

3.3. Electrical Conductivity. Electrical conductivity, being one of the important thermophysical properties of ILs is crucial for many electrochemical applications. It is a measure of ion transport, which is predominantly governed by the degree of dissociation of the ions, the viscosity, the ion mobility, aggregation of ions, and the ionic charge. Table 2 lists the electrical conductivities of the studied pure ILs over the temperature range from (293.15 to 333.15) K and at atmospheric pressure, which span over a range from (0.01 to 1) S·m^{-1} and show moderate conductivity as found in other ammonium- and pyridinium-based ILs in literature.[73,74] As can be seen from Figure 4, for all the studied ILs electrical

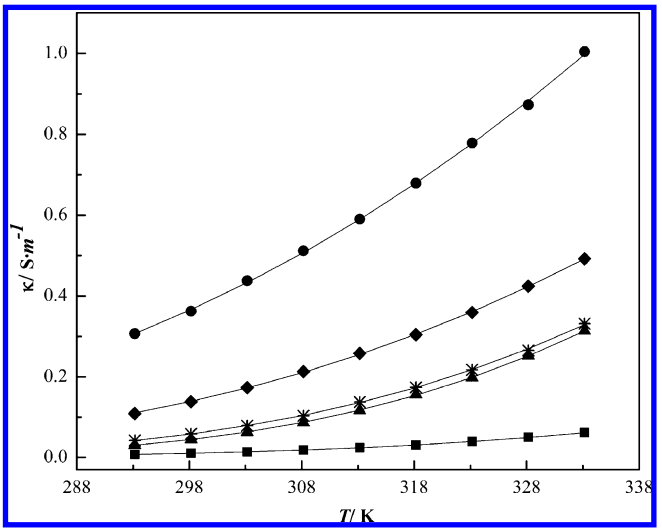

Figure 4. Experimental electrical conductivity values of ionic liquids as a function of temperature from (293.15 to 333.15) K: ●, PAF; ∗, AAc; ◆, 3HPAF; ■, 3HPAAc; ▲, 3HPATFAc. The symbols represent experimental values and the solid lines represent the values calculated from eq 12

conductivity increases with a rise in temperature probably due to the increase in mobility of ions. At any temperature, for instance at 298.15 K, formate-based ILs (PAF = 0.36 S·m^{-1}; 3HPAF = 0.14 S·m^{-1}) demonstrate better electrical conductivity than acetate-based ILs (PAA, 0.06 S·m^{-1}; 3HPAAc, 0.01 S·m^{-1}). The results are quite alike with that found in most of the literature which states that the electrical conductivity decreases with increasing alkyl chain length of ion.[75,76] The alkyl chain length does not largely affect the interaction energy between the cation and anion in the ILs, whereas the dispersion interactions between the alkyl chains in the liquid phase increase significantly, which renders the mobility of ions difficult. Furthermore, it can be seen from Table 2 that, upon functionalization of a cation with a hydroxyl group, the electrical conductivity decreases probably due to the ampihillic self-assembly nature of the hydroxyl group, as compared to their nonfunctionalized homologues.[10] A comparison of the electrical conductivity between 3HPAAc and 3HPATFAc shows that the latter possesses higher conductivity because of the presence of fluorine atoms which facilitates charge delocalization and in turn weakens the hydrogen bonding.[77] The measured electrical conductivities for 3HPAF and 3HPAAc at several temperatures are far less than that reported by Pinkert et al.[35] (water content: 6600 and 7200 ppm for 3HPAF and 3HPAAc, respectively), and slightly more for PAAc than that reported by Hou et al.[34] at 298.15 K (water content: 150 ppm); the literature values are illustrated in Table 2. The difference in electrical conductivity between measured values and those of Pinkert et al.[35] as shown in the Supporting Information (Figure S7) can be attributed mostly to the difference in water content, as it affects drastically the transport properties and, to some extent, the involvement of different measurement technique.

The temperature dependent electrical conductivity values were fitted to the nonlinear Vogel-Tamannn-Fulcher (VTF) equation.

DOI: 10.1021/acs.jced.5b00077
J. Chem. Eng. Data XXXX, XXX, XXX−XXX

$$\kappa = \kappa_0 \exp\left(\frac{-B}{T - T_0}\right) \quad (12)$$

where, κ_0, B, and T_0 are fitting parameters, and the values are illustrated in Table 6, along with ARD. The measured electrical conductivity values were used to calculate the molar conductivity by using the equation given below and the values are reported in Table 5.

$$\Lambda = \frac{\kappa M}{\rho} \quad (13)$$

The fractional Walden rule has proven to be a useful tool for gaining insight into the cation−anion interactions of ILs and expressed as the coupling behavior between molar conductivity and fluidity (reciprocal of viscosity) as given by eq 14.[78]

$$\log \Lambda = \log C + \alpha \log \eta^{-1} \quad (14)$$

where η^{-1} is the fluidity, and α represents the slope with the value equal to 1, corresponding to the ideal line. Therefore, α (the values are presented in Table 4) represents the qualitative measure of ionicity for the ionic liquids.[79] Figure 5 shows the Walden plot, where all the studied five ILs behave as that of less ionic in nature and fall below the ideal line. The ionicity follows the order 3HPATFAc > 3HPAF > 3HPAAc and PAF > PAAc, exactly as they followed for ΔpK_a (Table 4), obtained from the difference in pK_a between acids and bases. The observation is in good agreement with the results of Yoshizawa and Angell.[80]

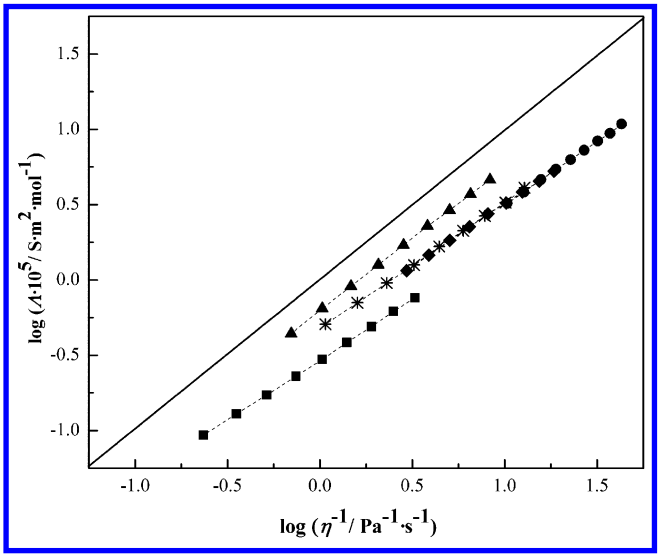

Figure 5. Molar conductivity against the fluidity (reciprocal of viscosity) for the studied PILs: ●, PAF; ∗, PAAc; ◆, 3HPAF; ■, 3HPAAc; ▲, 3HPATFAc. The solid line represents the Walden line with α = 1, and the dashed lines are only for guiding to eye.

4. CONCLUSIONS

The experimental study on surface tension, refractive index, and electrical conductivity in the temperature range from (293.15 to 333.15) K, shows that the cation, anion, and temperature have significant influence on thermophysical properties of studied PILs. The surface tension and refractive index decrease linearly, whereas, the electrical conductivity increases exponentially with increase in temperature. The measured values correlated well with the established empirical equations. In regard to surface ordering, the studied PILs show better surface entropy than the alkanes, which by far are considered as examples of surface organization. In the studied temperature range, the values of parachor, molar refraction, and electronic polarizability are found to be weakly dependent on temperature. Critical temperatures and boiling point temperatures were estimated from the semi-empirical Eötvos and Guggenheim equations, and the results indicate that functionalized PILs have lower volatility compared to their nonfunctionalized counterpart. The Walden products of these ILs were below the ideal line, and 3HPATFAc having the highest ionicity implies that the constituted ions could move more independently of one another. Upon the hydroxyl group substitution on cationic chain length, probably due to the polar nature of −OH, the surface tension and refractive index of ionic liquids increases significantly; however, the electrical conductivity behaves in a reverse manner. Moreover, with increasing anionic chain length, all of the experimental properties were found to be decreased. Fluorine-substituted ionic liquid, 3HPATFAc, providing far different results in each of the studied properties validates the tailoring ability of ILs to meet specific applications.

■ ASSOCIATED CONTENT

Supporting Information

The Supporting Information is available free of charge on the ACS Publications website at DOI: 10.1021/acs.jced.5b00077.

■ AUTHOR INFORMATION

Corresponding Author

*Tel.: +91 44 2257 4248. Fax: +91 44 2257 4202. E-mail: gardas@iitm.ac.in.

Notes

The authors declare no competing financial interest.

■ ACKNOWLEDGMENTS

The authors would like to acknowledge the Council of Scientific and Industrial Research (CSIR), Department of Science and Technology (DST), and IIT Madras for their financial support through Grant Nos. 01(2525)/11/EMR-II, SR/FT/CS-45/2011, and CHY/10-11/523/NFSC/RAME, respectively. Also the authors would like to thank Dr. Jitendra Sangwai, IIT Madras, India, and Dr. Naved Malek, SVNIT, Surat, India, for providing some facilities during experimental measurements.

■ REFERENCES

(1) Plechkova, N. V.; Seddon, K. R. Applications of Ionic Liquids in the Chemical Industry. *Chem. Soc. Rev.* **2008**, *37*, 123−150.

(2) Pinkert, A.; Marsh, K. N.; Pang, S.; Staiger, M. P. Ionic Liquids and Their Interaction with Cellulose. *Chem. Rev.* **2009**, *109*, 6712−6728.

(3) Dyson, P. J.; Geldbach, T. J. Applications of Ionic Liquids in Synthesis and Catalysis. *J. Electrochem. Soc. Interface* **2007**, *16*, 50−53.

(4) Chen, Q.-L.; Wu, K.-J.; He, C.-H. Thermal Conductivity of Ionic Liquids at Atmospheric Pressure: Database, Analysis, and Prediction Using a Topological Index Method. *Ind. Eng. Chem. Res.* **2014**, *53*, 7224−7232.

(5) Pandey, S.; Baker, S. N.; Pandey, S.; Baker, G. A. Optically Responsive Switchable Ionic Liquid for Internally-Referenced Fluorescence Monitoring and Visual Determination of Carbon Dioxide. *Chem. Commun.* **2012**, *48*, 7043−7045.

(6) Giernoth, R. Task-Specific Ionic Liquids. *Angew. Chem., Int. Ed.* **2010**, *49*, 2834−2839.

DOI: 10.1021/acs.jced.5b00077
J. Chem. Eng. Data XXXX, XXX, XXX−XXX

(7) Cole, A. C.; Jensen, J. L.; Ntai, I.; Tran, K. L. T.; Weaver, K. J.; Forbes, D. C.; Davis, J. H. Novel Brønsted Acidic Ionic Liquids and Their Use as Dual Solvent-Catalysts. *J. Am. Chem. Soc.* **2002**, *124*, 5962−5963.
(8) Kanzaki, R.; Uchida, K.; Song, X.; Umebayashi, Y.; Ishiguro, S. Acidity and Basicity of Aqueous Mixtures of a Protic Ionic Liquid, Ethylammonium Nitrate. *Anal. Sci.* **2008**, *24*, 1347−1379.
(9) Greaves, T. L.; Drummond, C. J. Protic Ionic Liquids: Properties and Applications. *Chem. Rev.* **2008**, *108*, 206−237.
(10) Greaves, T. L.; Weerawardena, A.; Krodkiewska, I.; Drummond, C. J. Protic Ionic Liquids: Physicochemical Properties and Behavior as Amphiphile Self-Assembly Solvents. *J. Phys. Chem. B* **2008**, *112*, 896−905.
(11) Reichert, E.; Wintringer, R.; Volmer, D. A.; Hempelmann, R. Electro-catalytic Oxidative Cleavage of Lignin in a Protic Ionic Liquid. *Phys. Chem. Chem. Phys.* **2012**, *14*, 5214−5221.
(12) Fernández-Castro, B.; Méndez-Morales, T.; Carrete, J.; Fazer, E.; Cabeza, O.; Rodríguez, J. R.; Turmine, M.; Varela, L. M. Surfactant Self-Assembly Nanostructures in Protic Ionic Liquids. *J. Phys. Chem. B* **2011**, *115*, 8145−8154.
(13) Gardas, R. L.; Coutinho, J. A. P. Group Contribution Methods for the Prediction of Thermophysical and Transport Properties of Ionic Liquids. *AIChE J.* **2009**, *55*, 1274−1290.
(14) Gardas, R. L.; Coutinho, J. A. P. A Group Contribution Method for Heat Capacity Estimation of Imidazolium-Based Ionic Liquids. *Ind. Eng. Chem. Res.* **2008**, *47*, 5751−5757.
(15) Gardas, R. L.; Coutinho, J. A. P. Applying a QSPR Correlation to the Prediction of Surface Tensions of Ionic Liquids. *Fluid Phase Equilib.* **2008**, *265*, 57−65.
(16) Nockemann, P.; Thijs, B.; Pittois, S.; Thoen, J.; Glorieux, C.; Van Hecke, K.; Van Meervelt, L.; Kirchner, B.; Binnemans, K. Task-Specific Ionic Liquid for Solubilizing Metal Oxides. *J. Phys. Chem. B* **2006**, *110*, 20978−20992.
(17) Tariq, M.; Freire, M. G.; Saramago, B.; Coutinho, J. A P.; Lopes, J. N. C.; Rebelo, L. P. N. Surface Tension of Ionic Liquids and Ionic Liquid Solutions. *Chem. Soc. Rev.* **2012**, *41*, 829−868.
(18) Gardas, R. L.; Ge, R.; Ab Manan, N.; Rooney, D. W.; Hardacre, C. Interfacial Tensions of Imidazolium-Based Ionic Liquids with Water and n-Alkanes. *Fluid Phase Equilib.* **2010**, *294*, 139−147.
(19) Wakeham, D.; Nelson, A.; Warr, G. G.; Atkin, R. Probing the Protic Ionic Liquid Surface Using X-ray Reflectivity. *Phys. Chem. Chem. Phys.* **2011**, *13*, 20828−20835.
(20) Deetlefs, M.; Seddon, K. R.; Shara, M. Neoteric Optical Media for Refractive Index Determination of Gems and Minerals. *New J. Chem.* **2006**, *30*, 317−326.
(21) MacFarlane, D. R.; Forsyth, M.; Howlett, P. C.; Pringle, J. M.; Sun, J.; Annat, G.; Neil, W.; Izgorodina, E. I. Ionic Liquids in Electrochemical Devices and Processes: Managing Interfacial Electrochemistry. *Acc. Chem. Res.* **2007**, *40*, 1165−1173.
(22) Ye, H.; Huang, J.; Xu, J. J.; Kodiweera, N. K. A. C.; Jayakody, J. R. P.; Greenbaum, S. G. New Membranes Based on Ionic Liquids for PEM Fuel Cells at Elevated Temperatures. *J. Power Sources* **2008**, *178*, 651−660.
(23) Menne, S.; Pires, J.; Anouti, M.; Balducci, A. Protic Ionic Liquids as Electrolytes for Lithium-Ion Batteries. *Electrochem. Commun.* **2013**, *31*, 39−41.
(24) Vogl, T.; Menne, S.; Balducci, A. Mixtures of Protic Ionic Liquids and Propylene Carbonate as Advanced Electrolytes for Lithium-Ion Batteries. *Phys. Chem. Chem. Phys.* **2014**, *16*, 25014−25023.
(25) Chhotaray, P. K.; Gardas, R. L. Thermophysical Properties of Ammonium and Hydroxylammonium Protic Ionic Liquids. *J. Chem. Thermodyn.* **2014**, *72*, 117−124.
(26) Yuan, X.; Zhang, S.; Liu, J.; Lu, X. Solubilities of CO_2 in Hydroxyl Ammonium Ionic Liquids at Elevated Pressures. *Fluid Phase Equilib.* **2007**, *257*, 195−200.
(27) Aparicio, S.; Atilhan, M.; Khraisheh, M.; Alcalde, R.; Fernandez, J. Study on Hydroxylammonium-Based Ionic Liquids. II. Computational Analysis of CO_2 Absorption. *J. Phys. Chem. B* **2011**, *115*, 12487−12498.
(28) Wang, C.; Luo, H.; Jiang, D.; Li, H.; Dai, S. Carbon Dioxide Capture by Superbase-Derived Protic Ionic Liquids. *Angew. Chem., Int. Ed.* **2010**, *49*, 5978−5981.
(29) Choi, H. M.; Kwon, I. Dissolution of Zein Using Protic Ionic Liquids: *N*-(2-Hydroxyethyl) Ammonium Formate and *N*-(2-Hydroxyethyl) Ammonium Acetate. *Ind. Eng. Chem. Res.* **2011**, *50*, 2452−2454.
(30) Bicak, N. A New Ionic Liquid: 2-Hydroxyethylammonium Formate. *J. Mol. Liq.* **2005**, *116*, 15−18.
(31) Zhao, B.; Greiner, L.; Leitner, W. Cellulose Solubilities in Carboxylate-Based Ionic Liquids. *R. Soc. Chem. Adv.* **2012**, *2*, 2476−2479.
(32) Chhotaray, P. K.; Jella, S.; Gardas, R. L. Physicochemical Properties of Low Viscous Lactam-Based Ionic Liquids. *J. Chem. Thermodyn.* **2014**, *74*, 255−262.
(33) Brandt, A.; Hallett, J. P.; Leak, D. J.; Murphy, R. J.; Welton, T. The Effect of the Ionic Liquid Anion in the Pretreatment of Pine Wood Chips. *Green Chem.* **2010**, *12*, 672−679.
(34) Hou, M.; Xu, Y.; Han, Y.; Chen, B.; Zhang, W.; Ye, Q.; Sun, J. Thermodynamic Properties of Aqueous Solutions of Two Ammonium-Based Protic Ionic Liquids at 298.15 K. *J. Mol. Liq.* **2013**, *178*, 149−155.
(35) Pinkert, A.; Ang, K. L.; Marsh, K. N.; Pang, S. Density, Viscosity and Electrical Conductivity of Protic Alkanolammonium Ionic Liquids. *Phys. Chem. Chem. Phys.* **2011**, *13*, 5136−5143.
(36) Santos, C. S.; Baldelli, S. Gas−Liquid Interface of Room-Temperature Ionic Liquids. *Chem. Soc. Rev.* **2010**, *39*, 2136−2145.
(37) Langmuir, I. Forces Near the Surfaces of Molecules. *Chem. Rev.* **1930**, *6*, 451−479.
(38) Rolo, L. I.; Cac, A. I.; Queimada, J.; Marrucho, I. M. Surface Tension of Heptane, Decane, Hexadecane, Eicosane, and Some of Their Binary Mixtures. *J. Chem. Eng. Data* **2002**, *47*, 1442−1445.
(39) Law, G.; Watson, P. R. Surface Orientation in Ionic Liquids. *Chem. Phys. Lett.* **2001**, *345*, 1−4.
(40) Jiang, W.; Wang, Y.; Yan, T.; Voth, G. A. A Multiscale Coarse-Graining Study of the Liquid/Vacuum Interface of Room-Temperature Ionic Liquids with Alkyl Substituents of Different Lengths. *J. Phys. Chem. C* **2008**, *112*, 1132−1139.
(41) Adamson, A. W.; Gast, A. P. *Physical Chemistry of Surfaces*, 6th ed.; John Wiley & Sons, Inc.: New York, 1997.
(42) Restolho, J.; Serro, A. P.; Mata, J. L.; Saramago, B. Viscosity and Surface Tension of 1-Ethanol-3-methylimidazolium Tetrafluoroborate and 1-Methyl-3-octylimidazolium Tetrafluoroborate over a Wide Temperature Range. *J. Chem. Eng. Data* **2009**, *54*, 950−955.
(43) Ghatee, M. H.; Bahrami, M.; Khanjari, N.; Firouzabadi, H.; Ahmadi, Y. A Functionalized High-Surface-Energy Ammonium-Based Ionic Liquid: Experimental Measurement of Viscosity, Density, and Surface Tension of (2-Hydroxyethyl)ammonium Formate. *J. Chem. Eng. Data* **2012**, *57*, 2095−2101.
(44) Fumino, K.; Wulf, A.; Ludwig, R. The Potential Role of Hydrogen Bonding in Aprotic and Protic Ionic Liquids. *Phys. Chem. Chem. Phys.* **2009**, *11*, 8790−8794.
(45) Sloutskin, E.; Bain, C. D.; Ocko, B. M.; Deutsch, M. Surface Freezing of Chain Molecules at the Liquid−liquid and Liquid−Air Interfaces. *Faraday Discuss.* **2005**, *129*, 339−352.
(46) Lynden-Bell, R. M. Gas−Liquid Interfaces of Room Temperature Ionic Liquids. *Mol. Phys.* **2003**, *101*, 2625−2633.
(47) Sloutskin, E.; Solutskin, E.; Ocko, B. M.; Tamam, L.; Taman, L.; Kuzmenko, I.; Gog, T.; Deutsch, M. Surface Layering in Ionic Liquids: An X-Ray Reflectivity Study. *J. Am. Chem. Soc.* **2005**, *127*, 7796−7804.
(48) Freire, M. G.; Carvalho, P. J.; Fernandes, A. M.; Marrucho, I. M.; Queimada, A. J.; Coutinho, J. A P. Surface Tensions of Imidazolium-Based Ionic Liquids: Anion, Cation, Temperature and Water Effect. *J. Colloid Interface Sci.* **2007**, *314*, 621−630.
(49) Poling, B. E.; Prausnitz, J. M.; O'Connell, J. P. *The Properties of Gases and Liquids*; McGraw-Hill: New York, 2001.

DOI: 10.1021/acs.jced.5b00077
J. Chem. Eng. Data XXXX, XXX, XXX−XXX

(50) Rebelo, L. P. N.; Canongia Lopes, J. N.; Esperança, J. M. S. S.; Filipe, E. On the Critical Temperature, Normal Boiling Point, and Vapor Pressure of Ionic Liquids. *J. Phys. Chem. B* **2005**, *109*, 6040−6043.
(51) Shereshefsky, L. Surface Tension of Saturated Vapors and the Equation of Eötvös. *J. Phys. Chem.* **1931**, *35*, 1712−1720.
(52) Guggenheim, E. A. The Principle of Correspondig States. *J. Chem. Phys.* **1945**, *13*, 253−261.
(53) Preiss, U. P. R. M.; Slattery, J. M.; Krossing, I. In Silico Prediction of Molecular Volumes, Heat Capacities, and Temperature-Dependent Densities of Ionic Liquids. *Ind. Eng. Chem. Res.* **2009**, *48*, 2290−2296.
(54) Deetlefs, M.; Seddon, K. R.; Shara, M. Predicting Physical Properties of Ionic Liquids. *Phys. Chem. Chem. Phys.* **2006**, *8*, 642−649.
(55) Gardas, R. L.; Rooney, D. W.; Hardacre, C. Development of a QSPR Correlation for the Parachor of 1,3-Dialkyl Imidazolium Based Ionic Liquids. *Fluid Phase Equilib.* **2009**, *283*, 31−37.
(56) Sugden, S. The Variation of Surface Tension with Temperature and Some Related Functions. *J. Chem. Soc. Trans.* **1924**, *125*, 32−41.
(57) Ma, X.-X.; Wei, J.; Zhang, Q.-B.; Tian, F.; Feng, Y.-Y.; Guan, W. Prediction of Thermophysical Properties of Acetate-Based Ionic Liquids Using Semiempirical Methods. *Ind. Eng. Chem. Res.* **2013**, *52*, 9490−9496.
(58) Prod'homme, L. A New Approach to the Thermal Change in the Refractive Index of Glasses. *Phys. Chem. Glasses.* **1960**, *1*, 119−122.
(59) Capelo, S. B.; Morales, T. M.; Carrete, J.; Lago, E. P.; Vila, J.; Cabeza, O.; Rodríguez, J. R.; Turmine, M.; Varela, L. M. Effect of Temperature and Cationic Chain Length on the Physical Properties of Ammonium Nitrate-Based Protic Ionic Liquids. *J. Phys. Chem. B* **2012**, *116*, 11302−11312.
(60) Hong, M.; Sun, A.; Liu, C.; Guan, W.; Tong, J.; Yang, J. Physico-Chemical Properties of 1 Alkyl-3-methylimidazolium Propionate Ionic Liquids {[$C_n$mim][Pro](n = 3, 4, 5, 6)} from 288.15 to 328.15 K. *Ind. Eng. Chem. Res.* **2013**, *52*, 15679−15683.
(61) Muhammad, N.; Man, Z. B.; Bustam, M. A.; Mutalib, M. I. A.; Wilfred, C. D.; Rafiq, S. Synthesis and Thermophysical Properties of Low Viscosity Amino Acid-Based Ionic Liquids. *J. Chem. Eng. Data* **2011**, *56*, 3157−3162.
(62) Tao, D.; Cheng, Z.; Chen, F.; Li, Z.; Hu, N.; Chen, X. Synthesis and Thermophysical Properties of Biocompatible Cholinium-Based Amino Acid Ionic Liquids. *J. Chem. Eng. Data* **2013**, *58*, 1542−1548.
(63) Seoane, R. G.; Corder, S.; Go, E.; Calvar, N.; Gonza, E. J.; Macedo, E. A.; Dominguez, A. Temperature Dependence and Structural Influence on the Thermophysical Properties of Eleven Commercial Ionic Liquids. *Ind. Eng. Chem. Res.* **2012**, *51*, 2492−2504.
(64) Meng, Y.; Liu, J.; Li, Z.; Wei, H. Synthesis and Physicochemical Properties of Two SO_3H-Functionalized Ionic Liquids with Hydrogen Sulfate Anion. *J. Chem. Eng. Data* **2014**, *59*, 2186−2195.
(65) Chen, Z. J.; Lee, J. Free Volume Model for the Unexpected Effect of C2-Methylation on the Properties of Imidazolium Ionic Liquids. *J. Phys. Chem. B* **2014**, *118*, 2712−2718.
(66) Hasse, B.; Lehmann, J.; Assenbaum, D.; Wasserscheid, P.; Leipertz, A.; Fröba, A. P. Viscosity, Interfacial Tension, Density, and Refractive Index of Ionic Liquids Dependence on Temperature at Atmospheric Pressure. *J. Chem. Eng. Data* **2009**, *54*, 2576−2583.
(67) Gutowski, K. E.; Maginn, E. J. Amine-Functionalized Task-Specific Ionic Liquids: A Mechanistic Explanation for the Dramatic Increase in Viscosity upon Complexation with CO_2 from Molecular Simulation. *J. Am. Chem. Soc.* **2008**, *130*, 14690−14704.
(68) Blanchard, L. A.; Gu, Z.; Brennecke, J. F. High-Pressure Phase Behavior of Ionic Liquid/CO_2 Systems. *J. Phys. Chem. B* **2001**, *105*, 2437−2444.
(69) Kilaru, P. K.; Scovazzo, P. Correlations of Low-Pressure Carbon Dioxide and Hydrocarbon Solubilities in Imidazolium-, Phosphonium-, and Ammonium-Based Room-Temperature Ionic Liquids. Part 2. Using Activation Energy of Viscosity. *Ind. Eng. Chem. Res.* **2008**, *47*, 910−919.
(70) Costa Gomes, M. F.; Pádua, A. A. Gas−Liquid Interactions in Solution. *Pure Appl. Chem.* **2005**, *77*, 653−665.
(71) Tariq, M.; Forte, P. a. S.; Gomes, M. F. C.; Lopes, J. N. C.; Rebelo, L. P. N. Densities and Refractive Indices of Imidazolium- and Phosphonium-Based Ionic Liquids: Effect of Temperature, Alkyl Chain Length, and Anion. *J. Chem. Thermodyn.* **2009**, *41*, 790−798.
(72) Fröba, A. P.; Kremer, H.; Leipertz, A. Density, Refractive Index, Interfacial Tension, and Viscosity of Ionic Liquids [EMIM][$EtSO_4$], [EMIM][NTf_2], [EMIM][$N(CN)_2$], and [OMA][NTf_2] in Dependence on Temperature at Atmospheric Pressure. *J. Phys. Chem. B* **2008**, *112*, 12420−12430.
(73) Makino, T.; Kanakubo, M.; Umecky, T.; Suzuki, A. Electrical Conductivities, Viscosities, and Densities of *N*-Acetoxyethyl-*N*,*N*-dimethyl-*N*-ethylammonium and *N*,*N*-Dimethyl-*N*-ethyl-*N*-methoxyethoxyethylammonium Bis(trifluoromethanesulfonyl)amide and Their Nonfunctionalized Analogues. *J. Chem. Eng. Data* **2013**, *58*, 370−376.
(74) Bandrés, I.; Montaño, D. F.; Gascón, I.; Cea, P.; Lafuente, C. Study of the Conductivity Behavior of Pyridinium-Based Ionic Liquids. *Electrochim. Acta* **2010**, *55*, 2252−2257.
(75) Fox, E. T.; Weaver, J. E. F.; Henderson, W. A. Tuning Binary Ionic Liquid Mixtures: Linking Alkyl Chain Length to Phase Behavior and Ionic Conductivity. *J. Phys. Chem. C* **2012**, *116*, 5270−5274.
(76) Tsuzuki, S. Factors Controlling the Diffusion of Ions in Ionic Liquids. *ChemPhysChem* **2012**, *13*, 1664−1670.
(77) Bagno, A.; Butts, C.; Chiappe, C.; D'Amico, F.; Lord, J. C. D.; Pieraccini, D.; Rastrelli, F. The Effect of the Anion on the Physical Properties of Trihalide-Based *N*,*N*-Dialkylimidazolium Ionic Liquids. *Org. Biomol. Chem.* **2005**, *3*, 1624−1630.
(78) Pan, Y.; Boyd, L. E.; Kruplak, J. F.; Cleland, W. E.; Wilkes, J. S.; Hussey, C. L. Physical and Transport Properties of Bis-(trifluoromethylsulfonyl)imide-Based Room-Temperature Ionic Liquids: Application to the Diffusion of Tris(2,2′-bipyridyl)ruthenium-(II). *J. Electrochem. Soc.* **2011**, *158*, F1−F9.
(79) MacFarlane, D. R.; Forsyth, M.; Izgorodina, E. I.; Abbott, A. P.; Annat, G.; Fraser, K. On the Concept of Ionicity in Ionic Liquids. *Phys. Chem. Chem. Phys.* **2009**, *11*, 4962−4967.
(80) Yoshizawa, M.; Xu, W.; Angell, C. A. Ionic Liquids by Proton Transfer: Vapor Pressure, Conductivity, and the Relevance of ΔpK_a from Aqueous Solutions. *J. Am. Chem. Soc.* **2003**, *125*, 15411−15419.

DOI: 10.1021/acs.jced.5b00077
J. Chem. Eng. Data XXXX, XXX, XXX−XXX